LHC BEAM LOSS MEASUREMENTS AND QUENCH LEVEL ABORT THRESHOLD ACCURACY

Bernd Dehning, Mariusz Sapinski, CERN, Geneva, Switzerland
Agnieszka Priebe, Poznan University of Technology, Poznan, Poland

Abstract

The LHC beam loss measurement system is designed to trigger the beam abort in case the magnet coil transition level from the superconducting to normal conducting sate is approached. The predicted heat deposition in the superconducting coils of the magnets have been determined by particle shower simulation codes, while for transient losses the enthalpy has been calculated. The results have been combined to determine the abort thresholds. Transient loss measurements of the energy depositions of lost protons with injected beams in the LHC are used to determine the accuracy of the beam abort threshold settings. The simulation predictions are reviewed and compared with the measurement results. The relative difference between measurements and simulation are between 30 to 50 %.

INTRODUCTION

Particle shower simulation have been performed in order to determine relation between energy deposition in the bending magnet coil and the signal outside the cryostat measured by ionisation chambers [1, 2]. The results of the simulation have been verified with the data taken during the first two beam-induced quenches. This comparison results in a first benchmark for the method of the beam loss monitor threshold settings. To study the accuracy of the Geant4 simulation transient losses have been used. For short losses ($< 10\mu s$) the heat transport in the helium has no effect and only the enthalpy of the coil cables is the relevant parameter. To disentangle geometrical effects from physical effects of the simulation code the homogeneous geometry in the centre of a 15 m long bending magnet has been chosen. The proton beam impact location at the beam screen (see Fig. 1, top) is in the horizontal or vertical plane, where the secondary particle shower is originating, reaching next the vacuum chamber (cold bore) and then the inner surface of the super conducting coil. The proton distribution on the inner side of the beam screen has a longitudinal width of $\sigma = 4\mathrm{m}$ (see Fig. 1, bottom) for LHC typical beam parameter at injection energy and at the location of bending magnets. The magnetic field in the coil of the magnet reaches on its inner surface (see Fig. 2, top) the highest values leading to quench margins at the inner coil surface which are smallest near the vertical plane (38 mJ/cm^3, see Fig. 2, bottom).

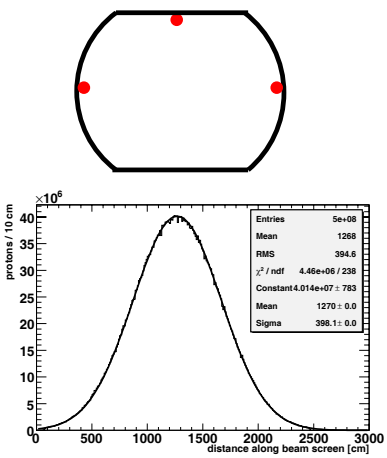

Figure 1: Top: Schematic view of the location of simulated beam losses on the beam screen (inside vacuum chamber). Bottom: Distribution of the lost protons along the beam screen of a single bunch ($4 \cdot 10^9$ proton) with transverse $\sigma_{\mathrm{beam}} = 1$ mm and an impact angle of 240 μrad.

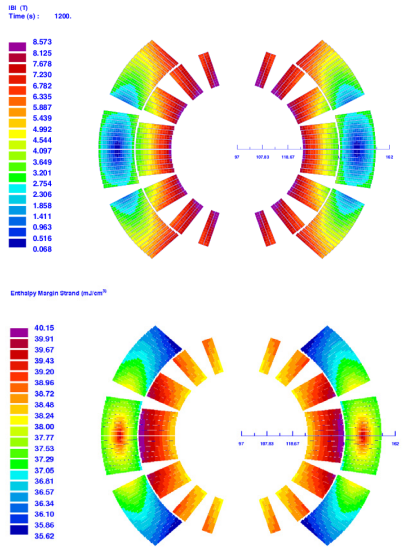

Figure 2: Top: Magnetic field at the coil of the MB magnet at collision energy (program: ROXIE [3]). Bottom: Quench margin at the cross section of the coil at injection energy [4].

PROTON SHOWER SIMULATIONS

The energy deposition in the different regions of the magnet and outside of the cryostat is recorded with an appropriate binning keeping the statistical errors smaller than the systematical. The highest energy deposition is observed at the beam screen reducing in radial direction for both planes ($E_{beam\_screen}/E_{first\_coil\_bin} = 25$ [1]). At the most exposed azimuth of the coil the maximum of the energy density deposition is reached after 0.3 to 0.5 m behind the impact location for both planes respectively (see

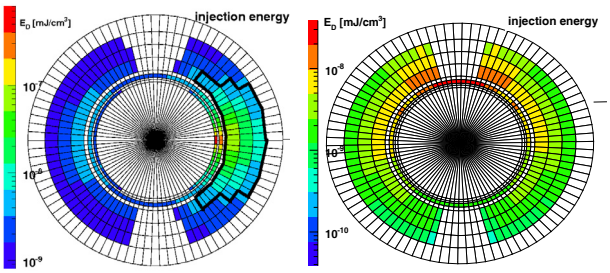

Figure 3: Cross section of bending magnet coil at the longitudinal position with maximum energy deposition (per proton, for point-like loss) at injection energy. Top: Horizontal loss with area containing 90% of the energy deposition (right site proton impact). Bottom: Vertical loss shower distribution (energy deposition in beam screen not shown).

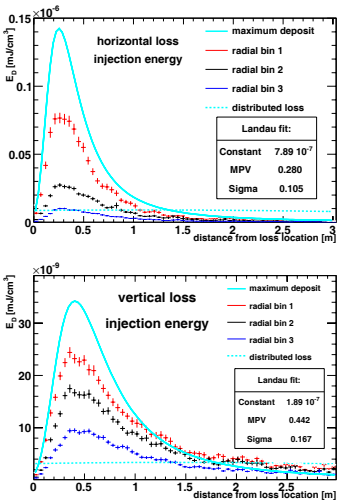

Figure 4: Longitudinal energy density distribution per impacting proton for the most exposed azimuth in the three cable layers (bins) of the inner coil (red being the innermost one and blue the outermost) as a function of distance from the loss location (top: horizontal, bottom: vertical loss). The blue continuous line represents the estimation of the maximum energy at the inner surface of the coil (Landau fit). The blue dashed line represents the expected energy deposition in case of distributed loss.

Fig. 4, top, bottom). The maximum of the horizontal loss is about 4 times larger than the maximum of the energy density of the vertical loss. This lower energy deposition could be explained by the distance of the coils to the vertical plane (see Fig. 3, bottom). The peak energy density at the inner surface of the coil for point losses is about 15 times larger than for distributed losses indicating the large smearing by the characteristic impact angle of 250 μrad and by the beam size of $\sigma_{beam\_arc} = 1mm$ (at 450 GeV). The shower particles are detected by the ionisation chambers tubes mounted at the outside surface of the cryostat. The shower particles leaving the cryostat and entering the chambers are almost perpendicular to the longitudinal axis (see Fig. 5) with a broad angular distribution ($\sigma = 30°$). The ionisation chambers sensitivity for different particle

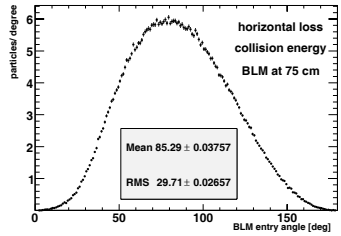

Figure 5: Angular distributions of particles entering a ionisation chamber at 75 cm from the loss location.

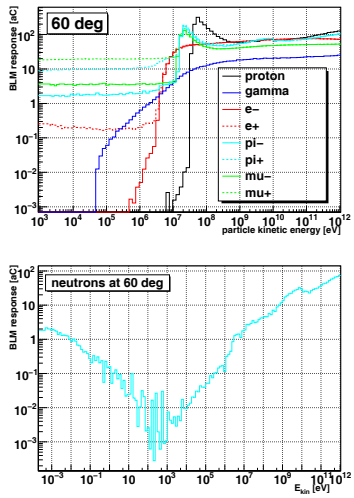

Figure 6: Response functions for 60° impact angle. Top: All considered particle types except neutrons. Bottom: Neutrons only.

types is characterised by its steep increase for protons at about 60 MeV and for pions at about 20 MeV (see Fig. 6, top). The muons, positrons and electrons show a less steep increase in the range between 10 to 60 MeV. For a kinetic particle energy larger than 400 MeV its sensitivity is almost constant for all of them. The photons show a much less steep increase and also their saturation value is about 5 times lower than the others. The neutrons chamber sensitivity is characterised by its high value at energies below 1 eV, its minimum at about 200 eV and its slow increase up to 100 aC as for other particles at 1 TeV (see Fig. 6, bottom). Taking the particle spectra (see [1]) and the re-

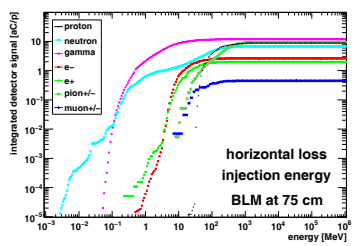

Figure 7: Ionisation chamber signal (per proton) as function of particle type and energy. The signals are integrated over the particle kinetic energy at a location of 75 cm behind the impact and deduced from the 60° response function.

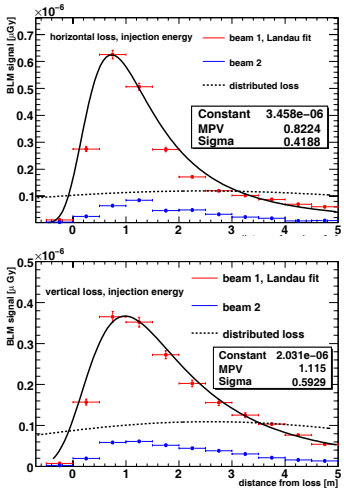

Figure 8: Signals per impacting proton in BLM cylinders along the cryostat as a function of distance from the loss location. Top: Injection beam energy, horizontal loss. Bottom: Injection beam energy, vertical loss.

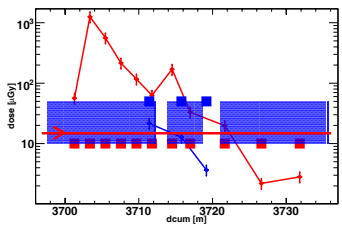

Figure 9: Beam loss signal profile for an impact of the proton beam with $2 \cdot 10^9$ protons in the centre of an bending magnet. Shown: the beam direction, the location of the monitors and the measurements.

sponse function into account the ionisation chamber signal is mainly generated by gammas, pions, protons and neutrons (see Fig. 7).

The simulated shower signal, which is intercepted by the ionisation chambers outside of the magnet cryostat peaks at about 1 m (in the coil at 0.3 to 0.5 m) behind the proton impact location (see Fig. 8, beam 1). The maximum of the horizontal loss is almost the same as the maximum for the vertical loss (in the coil this ratio is about 4). The maximum energy deposition for point losses is about 5 times larger than for distributed losses (in the coil is this factor 15). At the outside of the magnet the ratio between horizontal and vertical losses and point and distributed losses are strongly reduced compared to the situation in the coil. Ionisation chambers are installed on either side of the cryostat. Due to the different material thickness between impact position and ionisation chamber the signal ration is about 6 (see Fig. 8, beam 1, beam 2).

LOSS MEASUREMENTS

To verify the simulation results the injected beam has been directed towards the vertical centre of a bending magnet with ionisation chambers installed every 2.5 m (see Fig. 9). The loss signal reaches its maximum in the bending

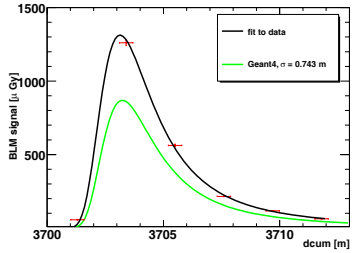

Figure 10: Second Quench causing loss signal with Landau fit curve and Geant 4 simulated ionisation chamber detector signals.

magnet and decreased towards the interconnection between bending magnet and quadrupole magnet. The first chamber at the quadrupole magnet registered an increased loss, because of the reduced shielding in between of the two magnets. Shown are also the losses measured with the ionisation chambers for the counter rotating beam (blue line). For comparison between measurements and simulations a loss scenario adapted simulation has been done (see Fig. 10). The loss measurements have been fitted with a Landau curve (black line) and the simulation result has been drawn (green line). The simulation underestimates the losses by 30 %. The simulated maximum energy density deposition at the inner surface of the coil is 15.6 mJ/cm^3, about 40 % of the enthalpy simulation result leading to a quench. Both discrepancies compensate each other partially in this case.

CONCLUSION

The Geant 4 simulations have been used to predict the energy deposition in the superconducting coils of the LHC magnets and at the outside mounted ionisation chambers. The energy depositions peaks and averages for the transverse longitudinal direction have been used to place the ionisation chambers at optimal positions. Particle spectra and detector response function have been used to determine the chamber signal response. The proton beam induced transient quench of a superconducting bending magnet has been used to determine the accuracy of Geant 4 simulation based threshold settings resulting in an accuracy of about 30 to 50 %.

REFERENCES

[1] B. Dehning, A. Priebe, M. Sapinski, "Energy deposition in LHC MB magnets and quench threshold test with beam, LHC Project Note 422, (2009).

[2] Future literature can be found: http://cern.ch/blm and at http://cern.ch/blm/talks_and_papers

[3] S. Russenschuck, "1st International Roxie Users Meeting and Workshop - ROXIE : routine for the optimization of magnet X-sections, inverse field calculation and coil end design, CERN yellow report 99-01, (1999).

[4] Nikolai Schwerg, priv comm.